First order perturbative calculations for a conducting liquid jet in a solenoid

J. Gallardo, S. Kahn, R. B. Palmer, P. Thieberger, R. Weggel
Brookhaven National Laboratory
Upton, NY 11973

K. McDonald
Princeton University
Princeton, NJ 08544

April 11, 2002

Abstract

A perturbative calculation is given of the behavior of a continuous jet of conducting fluid as it enters and leaves a solenoidal magnetic field. It is assumed that the changes in direction, jet cross section and velocity are small.

If the jet enters the field along, or close, to the axis, then the induced forces are compressive and retarding. The jet slows, suffers an increase in hydrostatic pressure, and increases in diameter; later, the jet re accelerates and elongates. As the jet leaves the field, the hydrostatic pressure becomes negative, and cavitation may occur.

If the jet enters at an angle to the axis, there are, in addition, deflections and elliptical deformations of the jet.

Formulae are given for these effects and numerical values given for the example of a solenoidal field with a Gaussian axial profile.

1 Introduction

A mercury jet, injected at an angle with respect to the axis of the solenoidal field, is the current baseline solution for the Feasibility Study II[1]. The interaction of the liquid-metal jet with the strong 20 T target solenoid has as result a number of forces on the jet which potentially may affect the viability of this target.[2] – [6] We present here perturbative calculations which confirm and extend the findings of previous authors.

2 Analytic Treatment

2.1 Introduction

The jet is assumed to have an initial radius r_o, and initial velocity v. Changes in radius, shape, direction and velocity are all assumed to be small. The angle between the jet and solenoid axes is also assumed to be small. Furthermore, we assume the jet to be very long $r_o \ll L$, and with zero viscosity.

In the following formulae, the coordinate system is defined by the jet; z is along the direction of motion and r is the radial coordinate.

If the jet is not directed along the solenoid axis, then we also define y in the plane of that axis and the jet and in a direction perpendicular to z (the jet axis) and away from the solenoid axis; and x perpendicular to y and z. We also define a second coordinate system x' y' z', where z' is aligned along the magnet axis. Assuming a small angle $\theta^2 << 1$ then (See Fig. 2.1):

$$\begin{aligned} x' &= x, \\ y' &\approx y_o + y + z\theta, \qquad (1) \\ z' &\approx z - (y + y_o)\theta \\ r'^2 &\approx r^2 + y_o^2 + 2yy_o + 2z\theta(y + y_o) \qquad (2) \end{aligned}$$

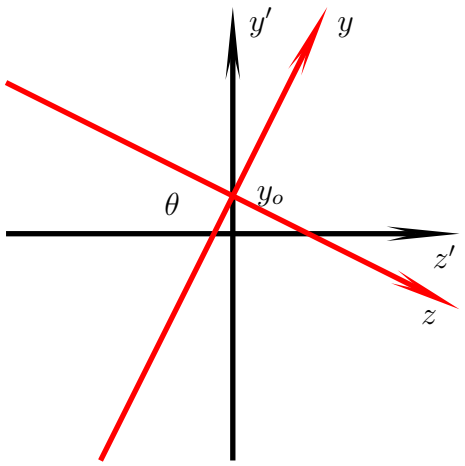

Figure 1: Schematic of the geometrical arrangement of solenoid and jet.

2.2 Induced azimuthal current

The magnetic flux through a circle of radius r perpendicular to the jet axis is

$$\Phi = \int_S dS\vec{n} \cdot \vec{B} \approx \pi r^2 B_z(x, y, z). \tag{3}$$

As a liquid metal jet passes axially down such a field at a velocity $v = dz/dt$, a circumferential potential will be generated

$$V \equiv \oint \vec{E} \cdot \vec{dl} = -\frac{d\Phi}{dt} = \pi r^2 v \frac{\partial B_z(x, y, z)}{\partial z}. \tag{4}$$

If the metal electrical conductivity κ is low enough so that the resulting current has a negligible effect on the field, then the azimuthal current density i_ϕ will be

$$i_\phi \approx \frac{V}{2\pi r}\kappa \approx -\frac{rv\kappa}{2}\frac{\partial B_z(0, 0, z)}{\partial z}. \tag{5}$$

2.3 Radial forces and hydrostatic pressure

The induced radial force per unit volume ($rdrd\phi dz$) is

$$f_r = B_z i_\phi \approx \frac{r}{2} v\kappa B_z \frac{\partial B_z}{\partial z}. \tag{6}$$

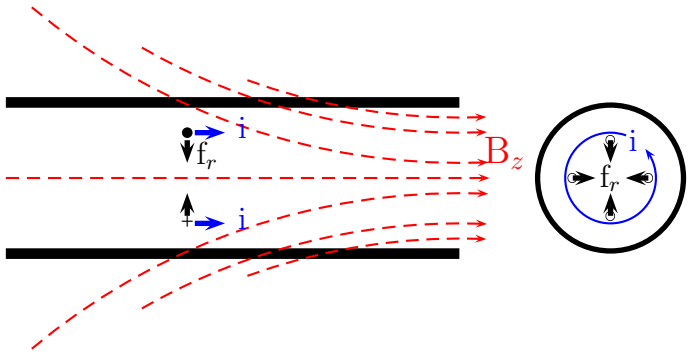

Figure 2: Radial pressure force produced by the axial magnetic field and the induced azimuthal current.

If we assume that the effects of the fields are small, so that the jet radius and liquid velocities do not vary by large fractions, and if we ignore radial inertia,

then the hydrostatic pressures in a jet of outside radius r_o, at radius r, will be given by

$$p(r,z) = \int_{r_o}^{r} -f_r dr \approx \left(\frac{r_o^2 - r^2}{4}\right)\ v\kappa\ B_z \frac{dB_z}{dz}. \tag{7}$$

2.4 Axial force

The above hydrostatic pressure is a function of z, and gradients in it will exert axial pressures f_p on the liquid that must be added to the magnetic term f_z.

$$f_p(\text{hydrostatic}) = \frac{\partial p(r,z)}{\partial z} \approx \ - \ \left(\frac{r_o^2 - r^2}{4}\right)\ v\kappa\ \frac{\partial}{\partial z}\left(B_z \frac{\partial B_z}{\partial z}\right). \tag{8}$$

To this must be added the axial forces induced directly by the fields acting on the asimuthal currents: If the jet is aligned with the field axis ($\theta = 0$), the

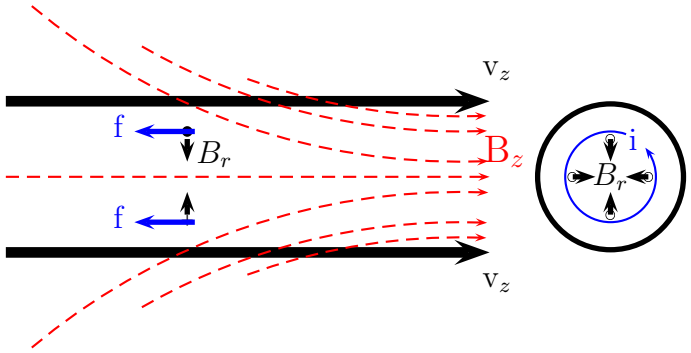

Figure 3: Retarding force in the axial direction

radial field is given by

$$B_r(\theta = 0) \approx -\frac{r}{2}\frac{\partial B_z(0,0,z)}{\partial z}. \tag{9}$$

The induced axial force per unit volume ($dr\ d\phi\ dz$) is

$$f_z(\theta = 0) = f_p(r,z) - B_r i_\phi. \tag{10}$$

If the jet is at an angle to the magnetic axis, then there is an additional shear force:

$$f_z(\theta) = f_p(r,z) - B_y i_\phi\ \sin(\phi) \quad \text{with} \quad B_y \approx \theta B_z(0,0,z), \tag{11}$$

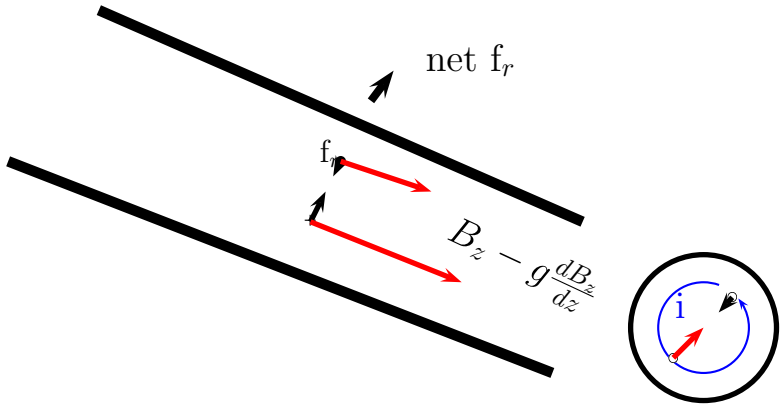

Figure 4: Deflection in the tilded case

giving, in all:

$$f_z \approx -\left(\frac{r_o^2 - r^2}{4}\right) v\kappa \frac{\partial}{\partial z}\left(B_z \frac{\partial B_z}{\partial z}\right) + \frac{r^2}{4} v\kappa \left(\frac{\partial B_z}{\partial z}\right)^2 + \frac{rv\kappa}{2} B_y \frac{\partial B_z}{\partial z} \sin\phi \quad (12)$$

On the jet axis:

$$f_z \approx -\left(\frac{r_o^2}{4}\right) v\kappa \frac{\partial}{\partial z}\left(B_z \frac{\partial B_z}{\partial z}\right). \quad (13)$$

On the outer surface, averaged over the azimuthal angle ϕ, or in the absence of B_y:

$$f_z \approx \frac{r_o^2}{4} v\kappa \left(\frac{\partial B_z}{\partial z}\right)^2. \quad (14)$$

On the outer surface, with a finite B_y, as in the case of a jet at an angle to the magnetic axis:

$$f_z \approx \frac{r_o^2}{4} v\kappa \left(\frac{\partial B_z}{\partial z}\right)^2 + \frac{y}{2} v\kappa \, B_y \, \frac{\partial B_z}{\partial z} \quad (15)$$

and the average force of the disk of radius r_o is given by integrating the terms

$$< f_z > \approx \frac{r_o^2}{8} v\kappa \left[\left(\frac{\partial B_z}{\partial z}\right)^2 + \frac{\partial}{\partial z}\left(B_z \frac{\partial B_z}{\partial z}\right)\right] \quad (16)$$

2.5 Axial accelerations

These forces will then decelerate, or accelerate layers of the fluid, thus inducing differences of liquid velocity as a function of radius

$$\frac{dv}{dz} = \frac{f}{\rho\, v} \tag{17}$$

where ρ is the fluid density.

$$\Delta\, v(r,z) = \int_{z_o}^{z} (f_z + f_p)\, \frac{1}{v\rho}\, dz \tag{18}$$

The average change in velocity is then

$$< \Delta v > (z) = \frac{\kappa}{\rho}\, \frac{r_o^2}{8} \left(\int_{z_o}^{z} \left(\frac{dB_z}{dz} \right)^2 + \frac{d}{dz} \left(B_z \frac{dB_z}{dz} \right) dz \right) \tag{19}$$

and the radius as a function of z is

$$r(z) = r_o \left(1 - \frac{< \Delta v > (z)}{v} \right) \tag{20}$$

2.6 Transverse forces and deflections

From Eq. 6, the radial force per unit volume ($dr\ r\ d\phi dz$) is $f_r = B_z i_\phi \approx \frac{r}{2}\, v\kappa\, B_z \frac{\partial B_z}{\partial z}$; if B_z varies with a transverse distance y, then the component of this radial force in the y direction is

$$f_y = f_r\ \sin\phi \tag{21}$$

and the net deflective force dF_y per unit length dz is

$$\frac{\partial F_y}{\partial z} = \int_0^r \int_0^{2\pi} \frac{r}{2}\, v\kappa\, \frac{\partial B_z}{\partial y}\, r \sin^2\phi \frac{\partial B_z}{\partial z}\, r\ dr d\phi \tag{22}$$

$$= \frac{v\kappa}{2}\, \frac{\partial B_z}{\partial y}\, \frac{\partial B_z}{\partial z} \int_0^{2\pi} \sin\phi^2 d\phi \int_0^r r^3\ dr \tag{23}$$

$$= \frac{\pi}{8} v\kappa\, r^4\, \frac{\partial B_z}{\partial y}\, \frac{\partial B_z}{\partial z}. \tag{24}$$

The change in transverse velocity is

$$\begin{aligned} \frac{\partial v_y}{\partial z} &= \frac{1}{v} \frac{\partial v_y}{dt} \\ &= \frac{\frac{dF_y}{dz} dz}{v\rho\pi r^2 dz} \\ &= \frac{\kappa r^2}{8\rho} \frac{\partial B_z}{\partial y} \frac{\partial B_z}{\partial z}. \end{aligned}$$

The inverse radius of bend is

$$\frac{d^2y}{dz^2} = \frac{d\theta}{dz} = \frac{\kappa\, r^2}{8\, v\, \rho}\, \frac{\partial B_z}{\partial y}\, \frac{\partial B_z}{\partial z}. \tag{25}$$

2.7 Induced axial current

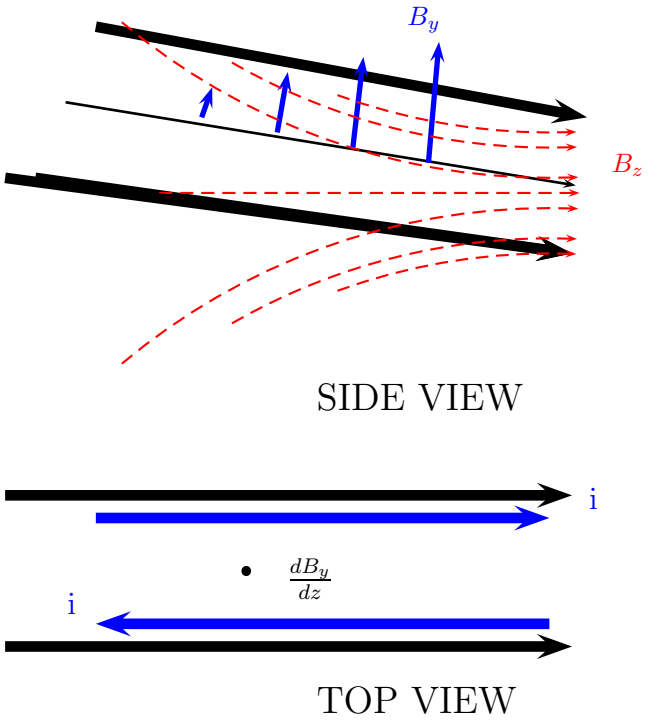

Figure 5: Induced axial current due to gradients in the radial field

Consider a transverse field component B_y
The magnetic flux between transverse positions $-x$ to x and dz is

$$d\Phi_y = 2xdzB_y(z) \tag{26}$$

As a liquid metal jet passes axially down such a field at a velocity $v = dz/dt$, axial voltage gradients will be generated

$$G = -x\frac{\partial B_y}{\partial z}v \tag{27}$$

If the metal electrical conductivity κ is low enough so that the resulting current has a negligible effect on the field, then the axial current density i_z will be

$$i_z = G\kappa = i_z \ = xv\kappa \frac{\partial B_y(0,0,z)}{\partial z} \tag{28}$$

2.8 Transverse elliptical distortion

If the jet is not on the solenoid axis, the axial induced currents interacting with the transverse fields will generate distorting forces on the jet. These transverse forces per unit volume $dx\ dy\ dz$ are

$$f_x \ = \ i_z \ B_y \ = \ x \ v \ \kappa \ B_y \ \frac{\partial B_y}{\partial z} \tag{29}$$

This force will distort the cross section. Assuming that the liquid is incompresible, we must find the induced pressures and motions $\Delta\vec{r}$ within the cross section that are driven by this force, with the constraint that the divergence of these motions is zero:

$$Div(\Delta\vec{r}) \ = \ 0 \tag{30}$$

Defining

$$F_o \ = \ v \ \kappa \ B_y \ \frac{\partial B_y}{\partial z}, \tag{31}$$

so that the magnet force per unit volume is

$$f_x(\text{magnetic}) \ = \ x \ F_o. \tag{32}$$

2.8.1 Magnetic Forces

The pressure on the surface of the jet will be independent of azimuthal angle ϕ

$$p(r_o)_{\text{circular}} = p_{\text{atm}} \ + \ T/r_o \ , \tag{33}$$

T being the surface tension. If the initial cross section is circular, we can consider pressures within the cross section:

$$p = p_o + r^2 \frac{F_o}{4}, \tag{34}$$

where p_o is set by the constraint on the above surface pressure at $r = r_o$. This bulk pressure will induce radial pressure forces:

$$f_r(\text{pressure}) = \frac{\partial p}{\partial r} = -\frac{rF_o}{2}; \tag{35}$$

so

$$f_x(\text{total}) = -\frac{F_o \ r \ \cos(\phi)}{2} \ = \ \frac{x \ F_o}{2}; \tag{36}$$

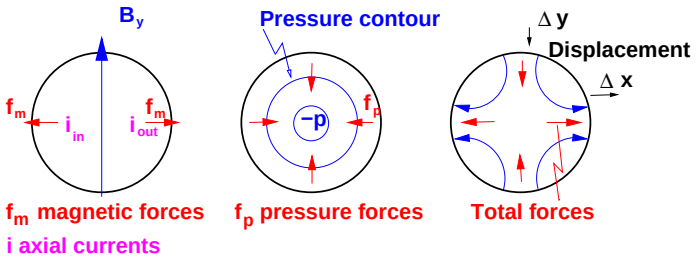

Figure 6: Distortion produced by the magnetic forces

$$f_y(\text{total}) \;=\; -\;\frac{F_o\; r\;\sin(\phi)}{2} \;=\; -\;\frac{y\;F_o}{2}. \tag{37}$$

The accelerations

$$\frac{d^2x,y}{dz^2} \;=\; \frac{f_{x,y}}{v^2\;\rho} \tag{38}$$

will give dispacements:

$$\Delta x \;=\; \int\int \frac{f_{x,y}}{v^2\;\rho}\;dz^2 \;=\; x\;\frac{\kappa}{2\;v\;\rho}\;\int\int\; B_y\;\frac{\partial B_y}{\partial z}\;dz^2, \tag{39}$$

$$\Delta y \;=\; \int\int \frac{f_{x,y}}{v^2\;\rho}\;dz^2 \;=\; -\,y\;\frac{\kappa}{2\;v\;\rho}\;\int\int\; B_y\;\frac{\partial B_y}{\partial z}\;dz^2. \tag{40}$$

Such motions are quadrupole (see Fig. 6) and, as required, give $Div\;(\Delta x, \Delta y) = 0$. The resulting ellipticity $\epsilon = \frac{\Delta x_o}{r_o} = -\frac{\Delta y_o}{r_o}$

$$\epsilon(z) \;=\frac{\kappa}{2v\rho}\;\int\int B_y\;\frac{\partial B_y}{\partial z}\;dz^2. \tag{41}$$

2.8.2 Surface tension forces

Once the cross section becomes somewhat elliptical (we consider only a small ellipticity), then the pressure at the surface is no longer independent of the asimuthal angle ϕ, but is given by:

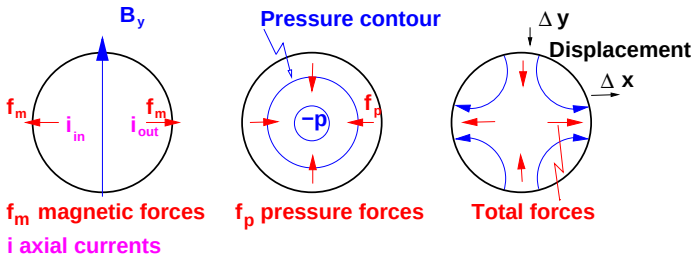

Figure 7: Restoring surface tension forces

$$p(r = r_o) \;=\; p_{\rm atm} \;+\; \frac{T}{r_0}\;(1 \;-\; \epsilon\;\cos(2\;\phi))\,. \tag{42}$$

Consider, in addition to those given above for the circular case, pressures within the cross section:

$$p(x,y)_{\rm elliptical} = p_o - \frac{T\epsilon}{r_o}\left(\cos^2(\phi) - \sin^2(\phi)\right) = p_o - \frac{T\epsilon}{r_o^3}(x^2 - y^2), \tag{43}$$

which has the correct values at $r = r_o$.

Defining

$$S_o \;=\; \frac{2\;T\;\epsilon}{r_o^3}, \tag{44}$$

the resulting bulk forces are:

$$f_x(\text{elliptical}) \;=\; \frac{\partial p}{\partial x} \;=\; x\;S_o, \tag{45}$$

$$f_y(\text{elliptical}) \;=\; \frac{\partial p}{\partial y} \;=\; -\,y\;S_o. \tag{46}$$

Once again, these are quadrupole forces that will generate quadrupole motions with Div($\Delta\vec{r}$)=0:

$$(\Delta x, \Delta y) = \int\int \frac{(x,\;-\,y)}{v^2\rho} S_o dz^2, \tag{47}$$

2.8.3 Magnetic and surface tension forces

Adding these surface tension displacements to the forces derived for the circular case:

$$(\Delta x, \Delta y) = (x, -y) \int\int \left(\frac{\kappa}{2\ v\ \rho}\ B_y\ \frac{\partial B_y}{\partial z}\ +\ \frac{2\ T\ \epsilon}{v^2\ \rho\ r_o^3} \right)\ dz^2, \tag{48}$$

and the resulting ellipticity $\epsilon = \frac{\Delta x_o}{r_o}\ =\ -\frac{\Delta y_o}{r_o}$:

$$\epsilon(z)\ =\ \int\int \left(\frac{r_o\ \kappa}{2\ v\ \rho}\ B_y\ \frac{\partial B_y}{\partial z}\ +\ \frac{2\ T\ \epsilon}{v^2\ \rho\ r_o^2} \right)\ dz^2. \tag{49}$$

3 Gaussian Case

We can consider a field that varies as a Gaussian in z. The fields of the solenoid and coordinates are denoted with primes ($'$).

The fields in the magnet system are:

$$B'_z(0,z') \approx B_o e^{-\frac{z'^2}{2\sigma_z^2}} \tag{50}$$

$$B'_z(r',z') \approx B'_z(0,z') - \frac{1}{4} r'^2 \frac{\partial^2 B'_z(0,z')}{\partial z'^2}, \tag{51}$$

$$B'_r(r',z') \approx -\frac{1}{2} r' \frac{\partial B'_z(0,z')}{\partial z'}. \tag{52}$$

In the coordinate system of the jet, see Fig. 2.1, assuming a very small angle θ, the fields are

$$\begin{aligned}
B_z(x,y,z) &\approx \left[B'_z(r',z') - \frac{1}{2}\theta\ y_o\ \frac{\partial B'_z(0,z')}{\partial z'} \right], \\
B_x(x,y,z) &\approx -\frac{1}{2} x \frac{\partial B'_z(0,z')}{\partial z'}, \\
B_y(x,y,z) &\approx -\left[\frac{1}{2}(y_o + z\theta) \frac{\partial B'_z(0,z')}{\partial z'} - \theta B'_z(r',z') \right], \\
\frac{\partial B_z(x,y,z)}{\partial z} &\approx \left[\frac{\partial B'_z(0,z')}{\partial z'} - \frac{1}{2}\ y_o\ \theta \frac{\partial^2 B'_z(0,z')}{\partial z'^2} \right], \\
\frac{\partial B_y(x,y,z)}{\partial z} &\approx \left[\frac{1}{2}\theta \frac{\partial B'_z(0,z')}{\partial z'}\ -\ \frac{1}{2}(\ y_o\ + z\theta) \frac{\partial^2 B'_z(0,z')}{\partial z'^2} \right].
\end{aligned} \tag{53}$$

4 Early Example

In our earlier studies we had considered a jet entering from outside the field, with the following parameters:

Table 1: Jet parameters for our earlier studies.

r_o (mm)	5
v_o (m/s)	20
θ (mrad)	100
σ_z (m)	0.6

Table 2: Summary of maximum and minimum values of the quantities shown in Fig. 8

B_z	Δp	$< \Delta v >$	Δv	Δy	Δx/r No ST	Δx/r
T	Atm.	m/s	m/s	mm	%	%
0.077	-0.245	-0.125	-5.542	-0.060	0.0	26
20.0	0.351	0.	0	0.045	423	-21

Using the above fomulae we obtain the results plotted in Figs. 8 and summarized in Tb. 2,

It is seen that although the deflection of the jet is small (0.04 mm) and the average deceleration is reasonable (0.125 m/s), yet there are several unacceptable results:

- The hydrostatic pressure falls to -0.24 atmosphers, and would require a high-pressure environment to stop the jet breaking up.
- There are shear accelerations of ± 5.5 m/s.
- The calculated distortion with surface tension included is 21% (without the surface tension it is 423%), indicating that the calculation is beyond its valid region, but suggesting that the jet will be badly disrupted.

Clearly these parameters are unacceptable.

5 Study II Example with $v = 30$ m/s

For Study II, several parameters were changed from the above example. The jet velocity increased, the magnetic field was kept more uniform, and the nozzle introduced inside the magnetic field.

The beam with rms radius $\sigma_r = 3$ mm intersects a mercury jet of radius r_o at an angle $\theta_{crossing}$. The forward velocity of the jet is v_o. The intervals between pulses is t, and it will be assumed here that after a pulse, all the mercury outside of the nozzle is dispersed. The nozzle is at z_{nozzle} with respect to the intersection of the beam and jet center lines. Consider the following parameters:

The geometry is shown in Fig. 9, with the distribution of resulting interactions as a function of z is shown above. At the time of a second, or subsequent bunch, the newly established jet will extend a distance $z_{jet} = v_o\, t = 0.6$ m from

Table 3: Proton beam and jet parameters for Study II example.

σ_r (mm)	1.5
r_o (mm)	5
$\theta_{crossing}$ (mrad)	33
v_o (m/s)	30
t (ms)	20
z_{nozzle} (m)	-0.375

Table 4: Hg jet parameters.

B_o (T)	20
σ'_z (m)	0.8
θ_{jet} (mrad)	-100
κ (Ω m)	10^6
ρ (kg/m^3)	13.5 10^4
$T_{\rm surface}$ (N/m)	0.456
$p_{\rm gas} = p_{\rm atmospheric}$ (N/m^2)	10^5

the nozzle. It is seen that only 2.5 % of the interactions would occur after this location, had the beam extended indefinitely. Thus there is a negligible loss from this limited jet extent.

Thus the total length over which the jet must propagate without serious magnetic disruption is from the nozzle to a point 0.6 m downstream. In order to minimize the field non uniformity over this length, the magnetic center (approximate point of maximum B_z is placed at the center of this length. *i.e.* the magnetic center is set at a distance $z_{magnet} = z_{jet}/2 - z_{nozzel} = -0.15$ m with respect to the jet-beam intersection.

The proton beam enters at an angle θ_{beam} with respect to the magnet axis. The jet is at an angle $\theta_{jet} = \theta_{beam} - \theta_{crossing}$. The vertical distance y_o from the magnet center ($z = 0, r = 0$) to the jet axis at $z = 0$ can be chosen to minimize beam disruption. We assume a Gaussian distribution of B'_z vs z', with a maximum value of B_o, The jet conductivity κ, density ρ, and surface tension $T_{surface}$, and the other parameters are given below:

Figures 10 use a horizontal scale with $z = 0$ at the magnetic center. Plots are shown for

a) The axial magnetic field B_z

b) The hydrostatic pressure on the jet axis with respect to the environment outside the jet ($p_{\rm axis} - p_{\rm gas}$)

c) The average deceleration of the jet Δ_v(Ave)

d) The maximum shear acceleration/deceleration of the upper/lower limits of the jet Δ_v(shear)

e) The vertical displacement of the jet due to deflecting forces y

g) The resulting elliptical distortion ($\Delta x/r = -\Delta y/r$), with and without surface tension.

We see that over the extent of the new jet (from - 0.3 to 0.3 m):

- The maximum axial field deviations are +/− 1.1 T = 5
- The axial pressure difference has a minimum of - 0.25 atmospheres. Thus if the jet is operating in a gas (He or Argon) at a pressure greater than or equal to 0.25 atmosphere, then the negative pressures will be avoided, and there will be no tendency to cavitate prior to the arrival of the beam.
- The maximum average deceleration of the jet is very small compared to the average jet velocity: 0.06/30≈0.2
- The maximum decelerations (from shear forces) are also small compared to the average jet velocity: 0.4/30≈1.3%.
- The deflections of the jet are very small: 5μm.
- The jet distortions (Δ width / ave width) are approximately 4% without surface tension, and less than 0.2% with surface tension.

Beyond the target region (z=0.3 to 1.5 m), the effects are larger, but still not sufficient to break up the jet. The maximum shear is about 5 m/sec, and the distortion 20 %. But these numbers are probably meaningless, since the jet will have been disrupted by the beam. These results are much better than in the earlier example and are considered to be acceptable.

We summarize in Tb. 5 these results

Table 5: Summary of maximum and minimum values of the quantities shown in Fig. 10

B_z	Δp	$< \Delta v >$	$\hat{\Delta v}$	Δy	Δx/r No ST	Δx/r
T	Atm.	m/s	m/s	mm	%	%
18.8	-0.240	0.0	-0.41	0.0	0.0	0.0
20.0	0.245	0.058	-0.019	0.005	0.37	0.18

6 Coil Design

The coil dimensions are given in Tb. 6.

The axial fields are shown in Figs. 11. The left figure shows the components from: the use of iron (green), superconductors (blue), and the total (red). The Gaussian distribution used in the above calculations is also given in Fig. 11-right (black), and is seen to be a good match to the total field over the target region (-0.6 m to 0).

Table 6: Coils used in the Study II target magnet [7]

len1 (m)	gap (m)	dl (m)	rad (m)	dr (m)	I/A (A/mm^2)	n I (A)	n I l (Am)
Fe							
0.980	0.980	0.108	0	0.313	0	0	0
1.088	0	0.312	0	0.168	0	0	0
Hollow							
1.288	-0.112	0.749	0.178	0.054	-24.37	0.98	1.26
1.288	-0.749	0.877	0.231	0.122	-19.07	2.04	3.74
1.288	-0.877	1.073	0.353	0.137	-14.87	2.18	5.78
SC							
0.747	-1.614	1.781	0.636	0.642	-23.39	26.77	160.95
2.628	0.100	0.729	0.686	0.325	-25.48	6.04	32.23
3.457	0.100	0.999	0.776	0.212	-29.73	6.29	34.86
4.556	0.100	1.550	0.776	0.107	-38.26	6.36	33.15
6.206	0.100	1.859	0.776	0.066	-49.39	6.02	30.59
8.000	-0.065	0.103	0.416	0.051	-68.32	0.36	1.00
8.275	0.172	2.728	0.422	0.029	-69.27	5.42	14.88
11.053	0.050	1.749	0.422	0.023	-75.62	3.00	8.18
12.852	0.050	1.750	0.422	0.019	-77.37	2.61	7.09
14.652	0.050	1.749	0.422	0.017	-78.78	2.30	6.22
16.451	0.050	1.750	0.422	0.015	-79.90	2.07	5.59
18.251	0.050	2.366	0.422	0.013	-80.85	2.53	6.80

7 Conclusion

- It is not acceptable to have the jet nozzle outside the magnetic field.
- With the Study II parameters, all disruptive effects are negligible up to the distance traveled by the jet since the last pulse.
- Even beyond this location, the disruptions are not unreasonable, and would not, of themselves, disrupt the jet.
- It would probably be acceptable to shorten the high field region, if this were desired for cost reasons.

References

[1] http://www.cap.bnl.gov/mumu/studyii/

[2] K. McDonald (Ed), *An R&D Program for Targetry and Capture at a Muon-Collider Source*, Proposal to the BNL AGS Division, p.23

[3] R. Weggel, *Behavior of conducting solid or liquid jet moving in magnetic field: 1) Paraxial; 2) Transverse; 3) Oblique*, BNL report BNL-65611/CAP-220-Muon-98R

[4] **Phys. Today**, Feb 2000, p.29

[5] K. McDonald, *Damping and Radial Pinching Effects*, http://www.hep.princeton.edu/~mcdonald/mumu/target/radialpinch.ps

[6] P. Thieberger, *Estimated perturbations of the axial motion of a liquid-metal jet entering a strong magnetic field* , MUC-NOTE-TARGET-0182, Nov. 2000.

[7] R. Weggel, *20 T Hybrid magnet for Study II*

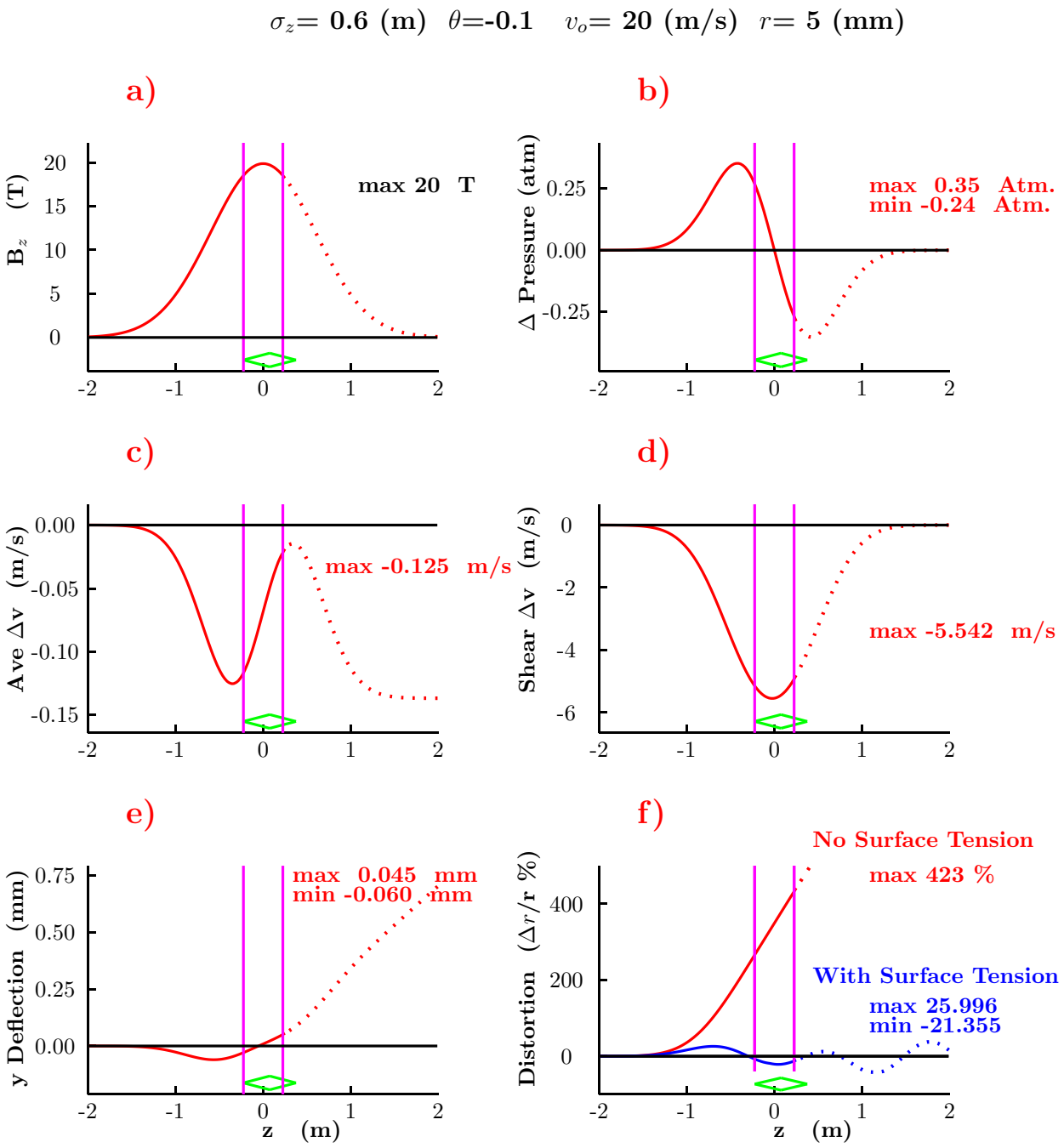

Figure 8: Results for the case of a jet entering a magnetic field with parameters listed in Tb. 1.

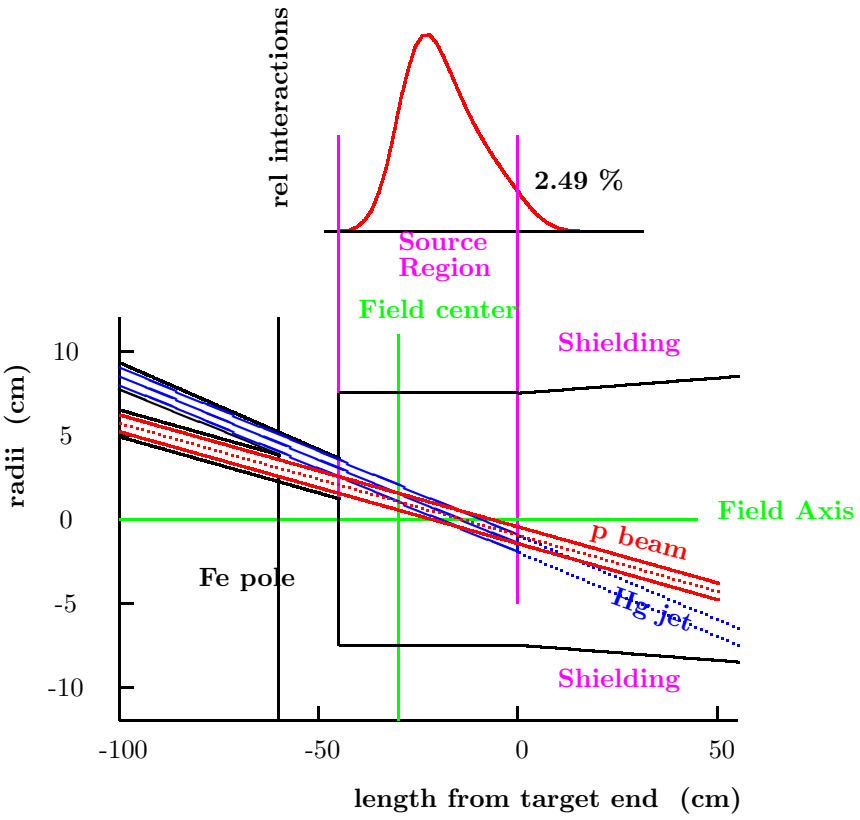

Figure 9: Geometry of the Hg jet, proton beam and target magnet; on top is the distribution of interactions as a function of z.

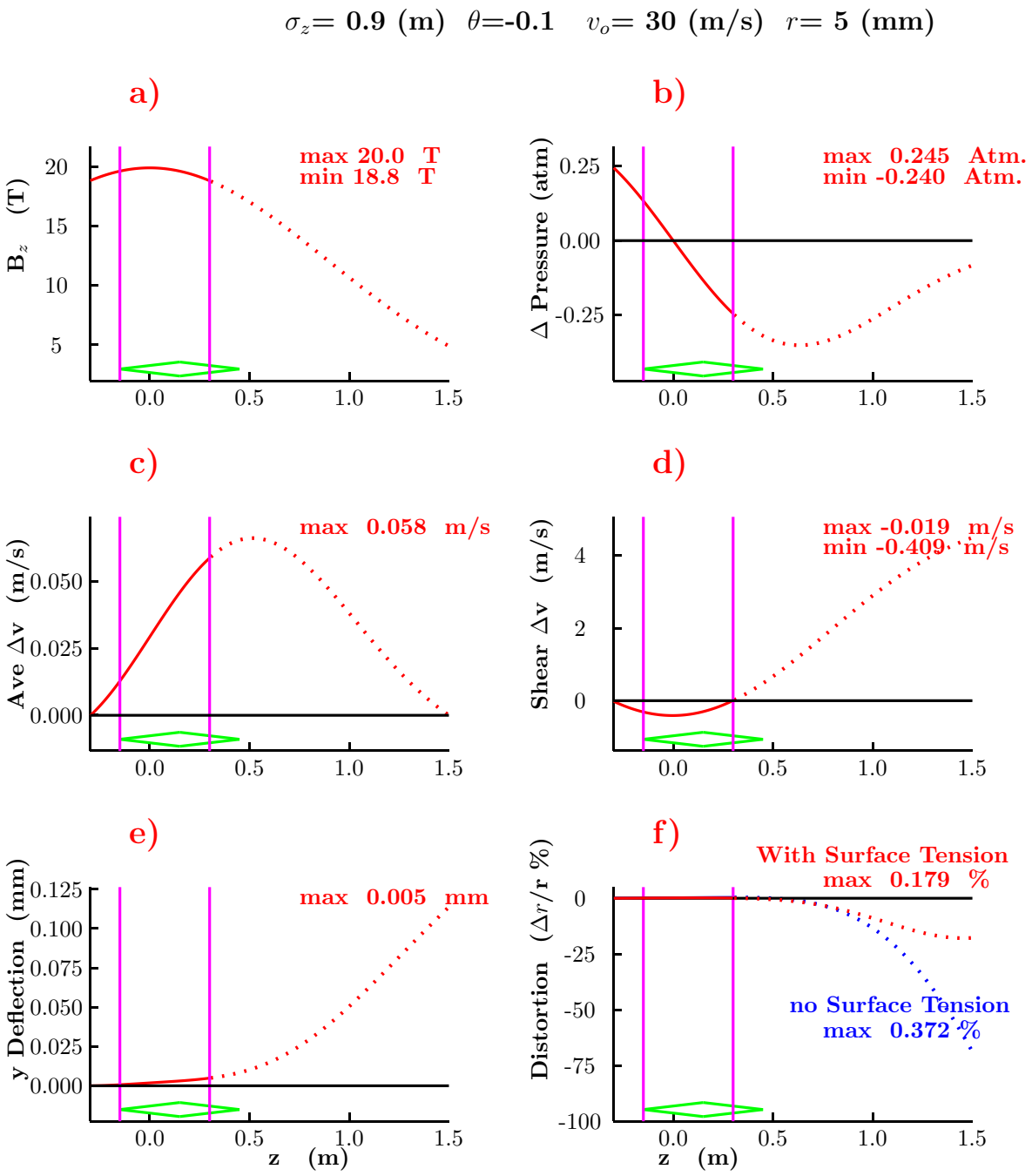

Figure 10: Results for the case of a jet with the noozle inside the magnetic field.

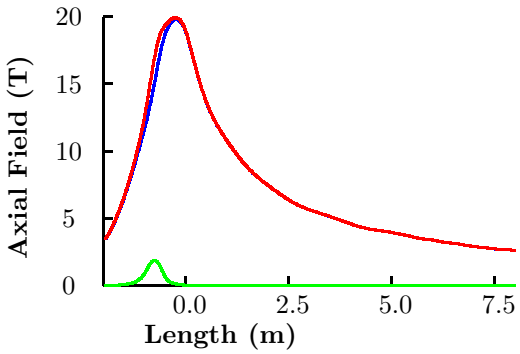
Axial Field (T)
20
15
10
5
0
0.0
2.5
5.0
7.5
Length (m)

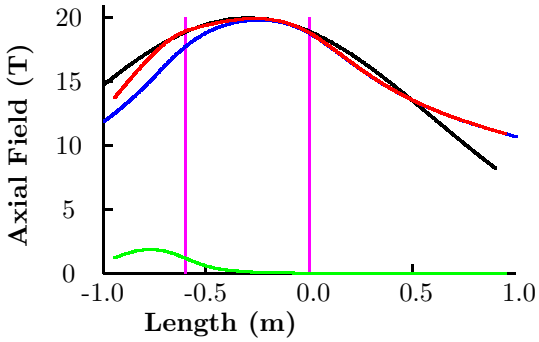
Axial Field (T)
20
15
10
5
0
-1.0
-0.5
0.0
0.5
1.0
Length (m)